

Electronic Supplementary Information

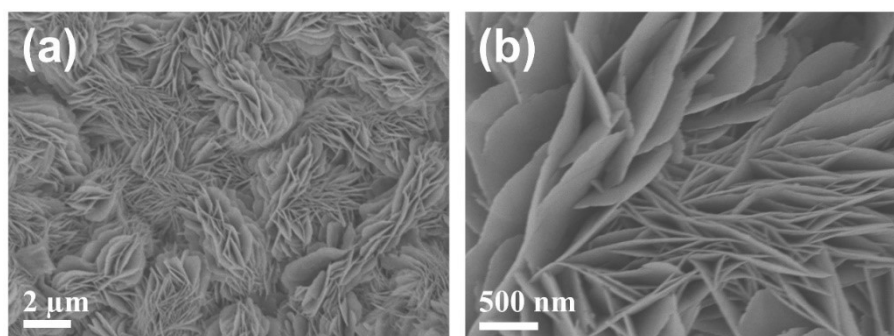


Fig. S1 SEM images of the NiRu-MOF/NF.

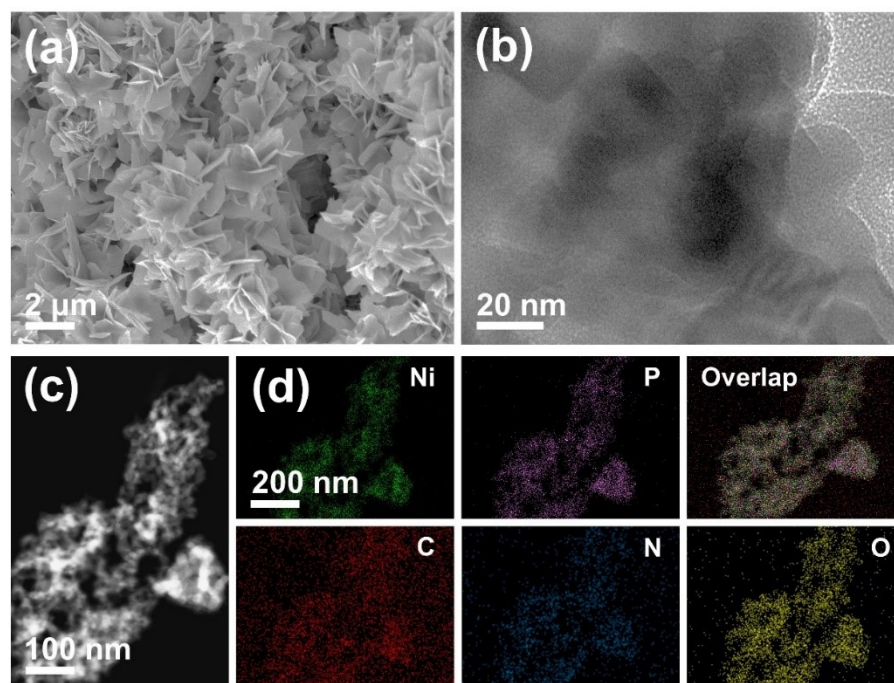


Fig. S2 (a) SEM image of the Ni_xP_y/N-C/NF. (b) TEM image, (c) HAADF-STEM image and (d) corresponding element mappings of the Ni_xP_y/N-C.

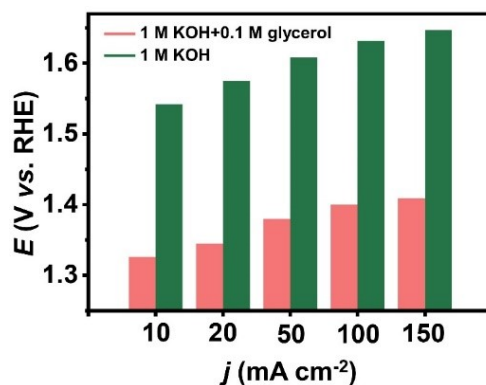


Fig. S3 Comparison of required applied potentials at different anodic current densities on the Ru-Ni_xP_y/N-C/NF electrode measured in 1 M KOH solution with and without 0.1 M glycerol.

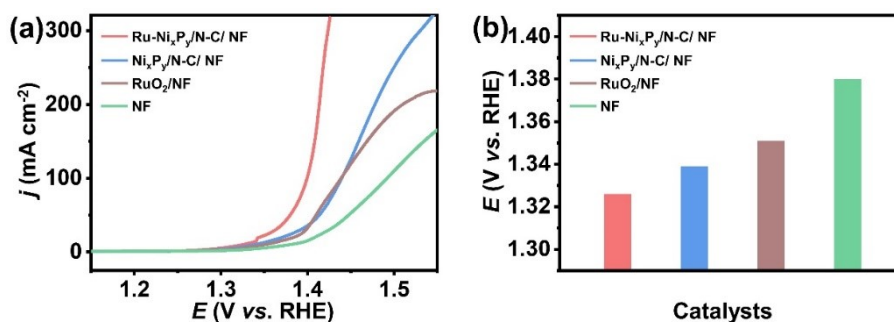


Fig. S4 (a) LSV curves measured in a 1.0 M KOH solution containing 0.1 M glycerol for Ru-Ni_xP_y/N-C/NF, Ni_xP_y/N-C/NF, RuO₂/NF and NF. (b) Comparison of required applied potentials at 10 mA cm⁻² for various catalysts.

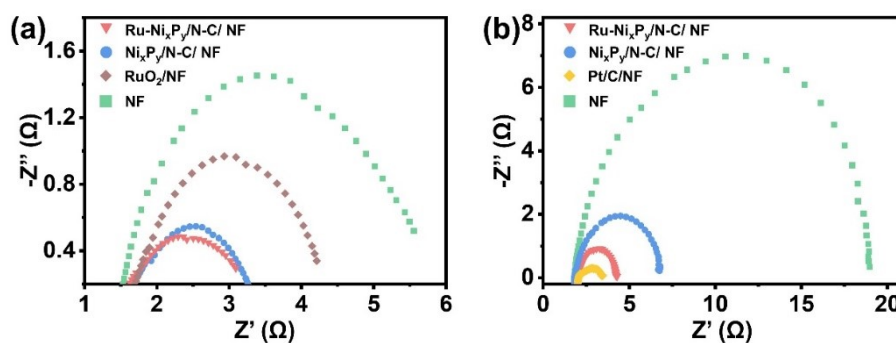


Fig. S5 Electrochemical impedance spectra of various catalysts in 1 M KOH solutions with and without 0.1 M glycerol and at different potentials: (a) 1.45 V (vs. RHE), with 0.1 M glycerol; (b) - 0.20 V (vs. RHE), without glycerol.

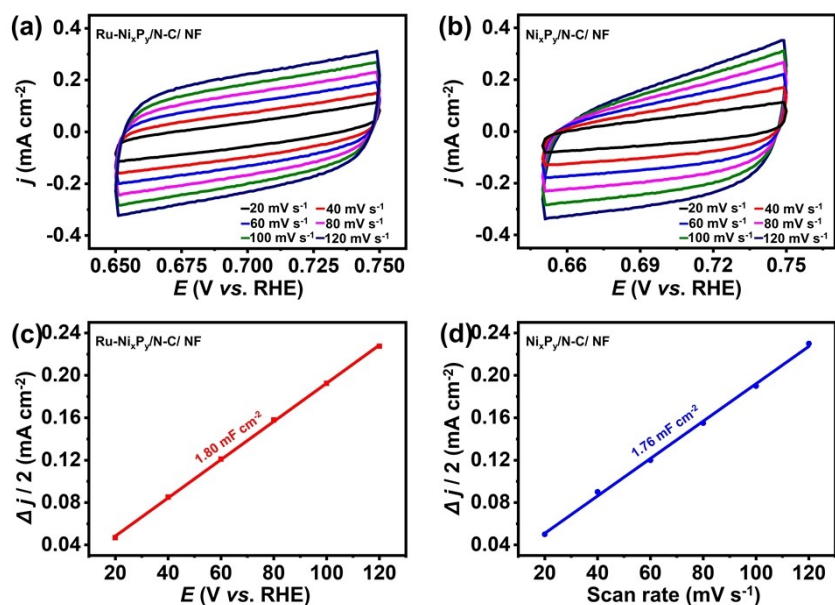


Fig. S6 Electrochemical C_{dl} measurements of (a) Ru-Ni_xP_y/N-C/NF and (b) Ni_xP_y/N-C/NF at scan rates of 20, 40, 60, 80, 100, and 120 mV s⁻¹. (c) Capacitance current density versus scan rate for (c) Ru-Ni_xP_y/N-C/NF and (d) Ni_xP_y/N-C/NF at 0.7 V (vs. RHE).

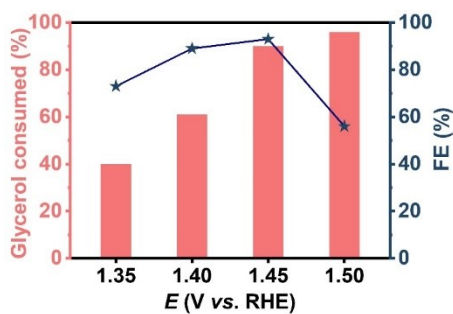


Fig. S7 Glycerol consumed and formate FE for Ru-Ni_xP_y/N-C/NF electrode at different potentials in a 1 M KOH solution containing 0.1 M glycerol.

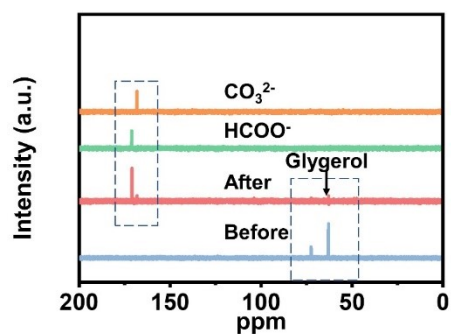


Fig. S8 The ^{13}C NMR spectra of the products of glycerol before and after 15 h of anodic oxidation, and the spectra of HCOO^- and CO_3^{2-} .

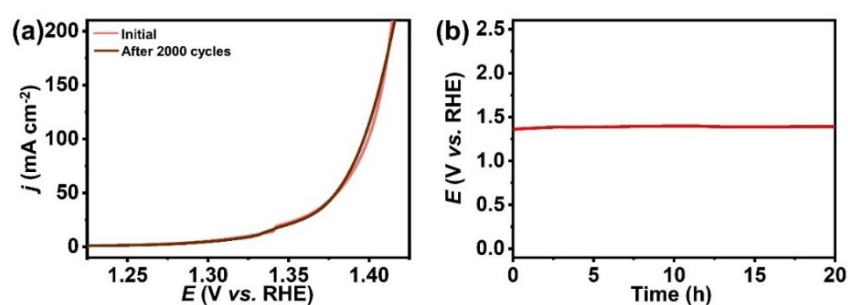


Fig. S9 (a) GOR polarization curves of $\text{Ru-Ni}_x\text{P}_y/\text{N-C/NF}$ at initial and after 2000 cycles. A fresh 1 M KOH solution containing 0.1 M glycerol was used when reported the LSV plot of 2000th cycle. (b) The V-t curves of $\text{Ru-Ni}_x\text{P}_y/\text{N-C/NF}$ measured at 10 mA cm^{-2} for 20 h (without iR compensation).

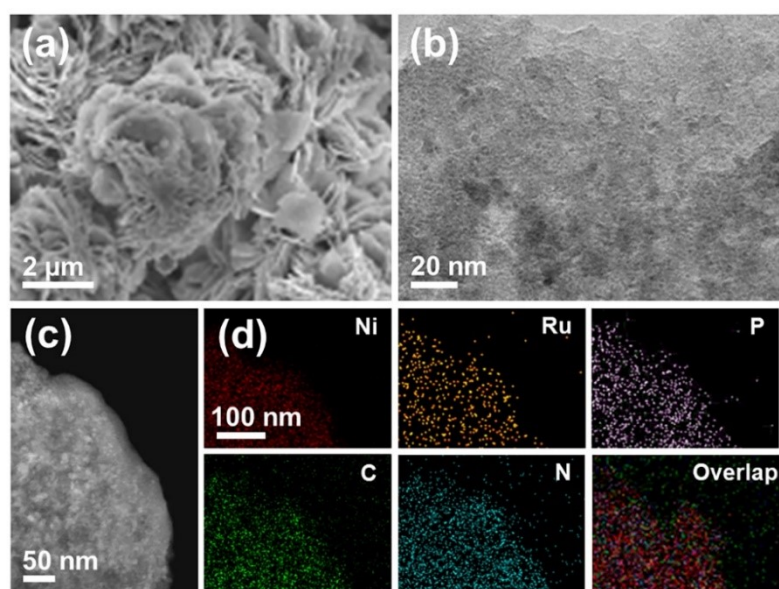


Fig. S10 (a) SEM of post-HER $\text{Ru-Ni}_x\text{P}_y/\text{N-C/NF}$. (b) TEM, (c) HAADF-STEM and (d) corresponding element mappings of the post-GOR $\text{Ru-Ni}_x\text{P}_y/\text{N-C}$.

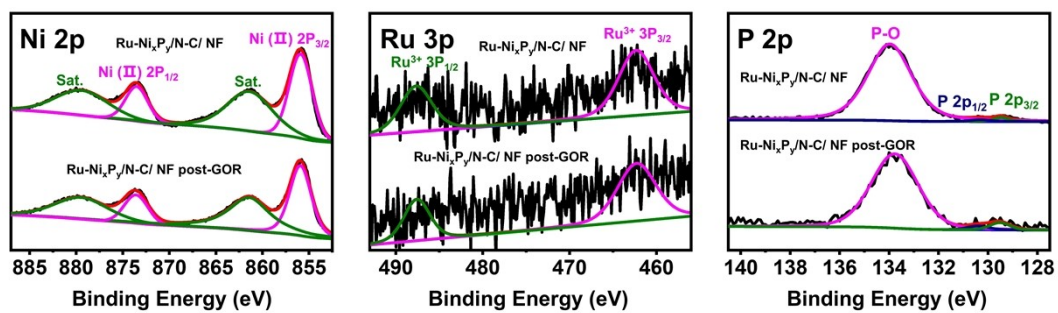


Fig. S11 (a) Ni 2p, (b) Ru 3p and (c) P 2p XPS spectra of fresh and post-GOR Ru-Ni_xP_y/N-C samples.

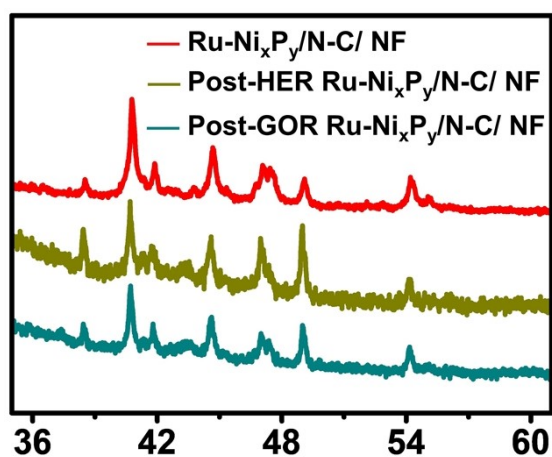


Fig. S12 XRD patterns of fresh, post-GOR and post-HER Ru-Ni_xP_y/N-C samples.

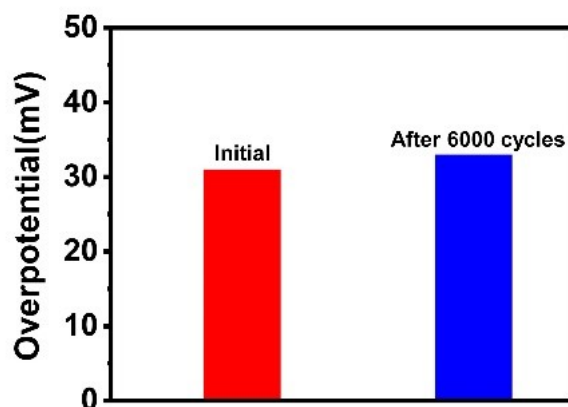


Fig. S13 Comparison of required overpotentials at a HER current density of 10 mA cm⁻² for Ru-Ni_xP_y/N-C/NF before and after 6000 cycles.

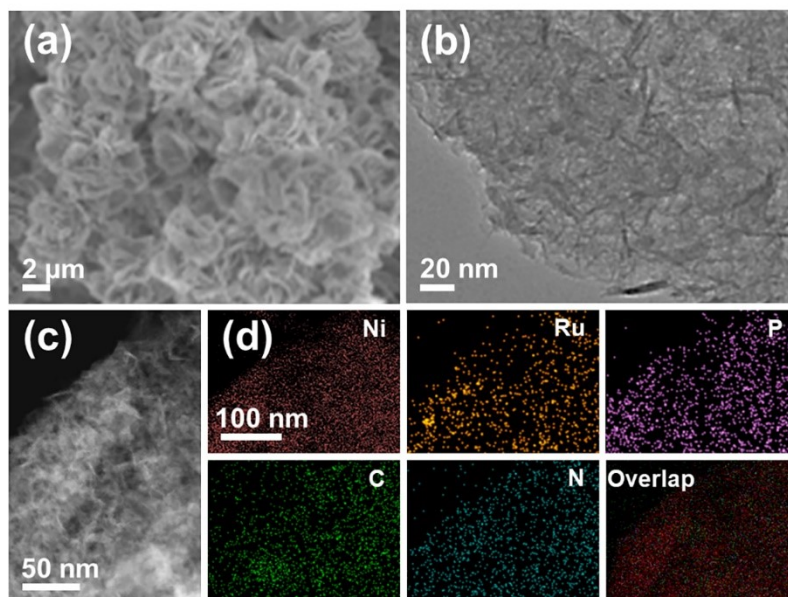


Fig. S14 (a) SEM of post-HER Ru-Ni_xP_y/N-C/NF. (b) TEM, (c) HAADF-STEM and (d) corresponding element mappings of the post-HER Ru-Ni_xP_y/N-C.

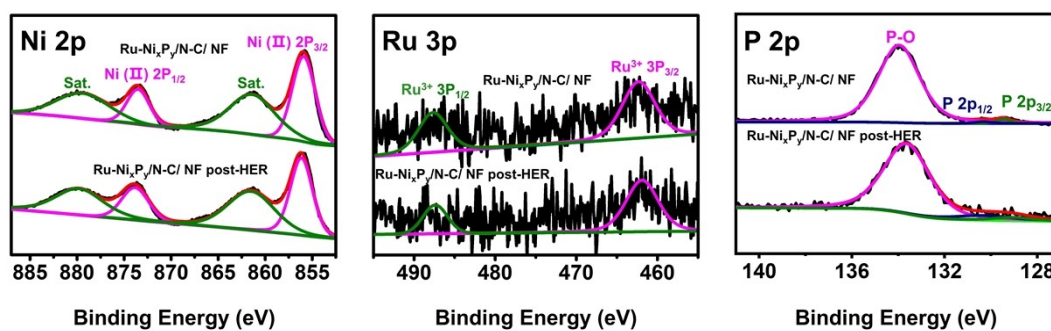


Fig. S15 (a) Ni 2p, (b) Ru 3p and (c) P 2p XPS spectra of fresh and post-HER Ru-Ni_xP_y/N-C samples.

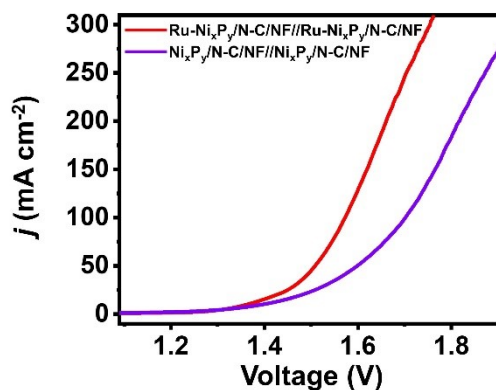


Fig. S16 LSV plots for Ru-Ni_xP_y/N-C/NF//Ru-Ni_xP_y/N-C/NF system and Ni_xP_y/N-C/NF//Ni_xP_y/N-C/NF in a 1 M KOH solution with 0.1 M glycerol.

Table S1. Comparison of the hydrogen evolution and organic electrosynthesis performance of our Ru-Ni_xP_y/N-C/NF||Ru-Ni_xP_y/N-C/NF system and other reported bifunctional catalyst-based co-electrolysis systems.

Bifunctional catalysts	Electrolyte	Main anode product	Cell voltage at 10 mA cm⁻² (V)	Ref.
Ru-Ni_xP_y/N-C/NF	1 M KOH+ 0.1 M glycerol	Formate	1.36	This work
NC/Ni-Mo-N/NF	1.0 M KOH+ 0.1 M glycerol	Formate	1.38	1
Ni ₃ S ₂ /NF	1M KOH + 0.01 M 5-hydroxymethylfurfural	2,5-furandicarboxylic acid	1.46	2
Ni ₂ P-UNMs/NF	1 M KOH + 0.125 M benzylamine	Benzonitrile	1.41	3
NiIr-MOF/NF	1 M KOH +4 M methanol	Formate	1.39	4
Ni(OH) ₂ /NF	1 M KOH + 0.5 M methanol	Formate	1.52	5
Ni _{0.33} Co _{0.67} (OH) ₂ /NF	1 M KOH + 0.5 M methanol	Formate	1.5	6
Co ₃ S ₄ -NSs/Ni-F	1.0 M KOH + 0.5 M ethanol	Acetate	1.48	7
Co-Ni alloy	1 M KOH + 0.1 M glucose	Gluconolactone, gluconic	1.39	8
Co-S-P/CC	1.0 M KOH + 1.0 M ethanol	Acetic acid	1.63	9

References

1. Y. Xu, M. Liu, S. Wang, K. Ren, M. Wang, Z. Wang, X. Li, L. Wang, H. Wang, *Appl. Cataly. B Environ.*, 2021, **298**, 120493.
2. B. You, X. Liu, N. Jiang, Y. Sun, *J. Am. Chem. Soc.*, 2016, **138**, 13639-13646.
3. Y. Ding, B.-Q. Miao, S.-N. Li, Y.-C. Jiang, Y.-Y. Liu, H.-C. Yao, Y. Chen, *Appl. Cataly. B Environ.*, 2020, **268**, 118393.
4. Y. Xu, M. Liu, M. Wang, T. Ren, K. Ren, Z. Wang, X. Li, L. Wang, H. Wang, *Appl. Cataly. B Environ.*, 2022, **300**, 120753.
5. J. Hao, J. Liu, D. Wu, M. Chen, Y. Liang, Q. Wang, L. Wang, X.-Z. Fu, J.-L. Luo, *Appl. Cataly. B Environ.*, 2021, **281**, 119510.
6. M. Li, X. Deng, K. Xiang, Y. Liang, B. Zhao, J. Hao, J.L. Luo, X.Z. Fu, *ChemSusChem.*, 2020, **13**, 914-921.
7. Y. Ding, Q. Xue, Q.L. Hong, F.M. Li, Y.C. Jiang, S.N. Li, Y. Chen, *ACS. Appl. Mater. Inter.*, 2021, **13**, 4026-4033.
8. C. Lin, P. Zhang, S. Wang, Q. Zhou, B. Na, H. Li, J. Tian, Y. Zhang, C. Deng, L. Meng, J. Wu, C. Liu, J. Hu, L. Zhang, *J. Alloy. Compd.*, 2020, **823**, 153784.
9. S. Sheng, K. Ye, L. Sha, K. Zhu, Y. Gao, J. Yan, G. Wang, D. Cao, *Inorg. Chem. Front.*, 2020, **7**, 4498-4506.